

# Impact of Battery Sizing on Stochastic Optimal Power Management in Plug-in Hybrid Electric Vehicles

Scott J. Moura, Duncan S. Callaway, Hosam K. Fathy, Jeffrey L. Stein

**Abstract**—This paper examines the impact of battery sizing on the performance and efficiency of power management algorithms in plug-in hybrid electric vehicles (PHEVs). Existing studies examine this impact for power management algorithms derived using either rule-based or deterministic dynamic programming methods. This paper extends the above investigations to power management algorithms optimized using stochastic dynamic programming (SDP). The paper treats both PHEV trip duration and PHEV power demand over the course of a given trip as stochastic. Furthermore, the paper examines two power management optimization objectives: one emphasizing fuel consumption only, and one that emphasizes the total cost of the *blended* use of fuel and electricity. The paper shows that blending provides significant benefits for small batteries, but this effect diminishes with increasing battery size.

## I. INTRODUCTION

THIS paper examines plug-in hybrid electric vehicles (PHEVs), which typically utilize onboard battery storage to at least partially displace liquid fuels with less expensive grid electricity. Battery sizing and design plays a key role in the cost, reliability, and ability of such PHEVs to effectively manage different power demand levels over the course of a diverse set of trip durations [1]. The goal of this paper is to examine the interplay between battery sizing and PHEV power management, specifically by quantifying the extent to which different PHEV power management algorithms enable the use of smaller batteries without compromising performance and efficiency. This quantification focuses on two power management algorithms: one that minimizes fuel consumption, and one that optimally *blends* fuel and electricity usage. The performance and efficiency characteristics of these algorithms are compared for different battery sizes over stochastic distributions of drive cycle trajectories and trip durations.

Previous work has investigated PHEV battery sizing from several different perspectives, including drive cycle requirements [2]-[4] and control design [4]-[6]. The results

of this previous research show that existing battery technologies possess the power-to-energy characteristics necessary to achieve all-electric ranges of up to 60km, at least for certain federally mandated drive cycle trajectories (e.g., FTP-72, HWFET, US06) [2], [3]. However, the literature also shows that operating PHEVs in an all-electric depletion mode often requires batteries with both high energy and high power characteristics, thus resulting in more expensive components [2], [4], [5]. This motivates the use of smaller batteries in combination with “*blending*” control strategies that utilize engine power throughout the depletion process to ration battery energy. The potential of such blending is evident from research by O’Keefe and Markel in which PHEV power management was explicitly optimized for fuel consumption over some known drive cycle using deterministic dynamic programming (DDP). This optimization furnished a control trajectory that blends battery and fuel usage such that the minimum battery energy level is achieved exactly when the trip terminates [6]. To summarize, the literature demonstrates the potential of applying blending control algorithms to reduce battery size requirements and thus PHEV acquisition costs, using both rule-based and DDP-based control methods.

In the survey provided above, the authors generally evaluate battery performance characteristics for specific drive cycles and trip durations. This paper provides two new contributions to this body of literature. First, it builds on previous work by the authors [7] to establish a framework for assessing PHEV performance using stochastic drive cycle models operated over a distribution of trip durations derived from real-world survey data. Secondly, it explicitly uses the monetary costs of fuel and electricity as objective functions in PHEV power management optimization, thereby establishing the machinery for a rigorous study on the tradeoffs between battery, fuel, and electricity costs in PHEVs. The paper’s results indicate that a blending strategy enables the use of smaller battery sizes, thus supporting the claims previously made in the literature.

The remainder of the paper is organized as follows: Section II introduces the vehicle configuration and models for the PHEV, daily travel time distributions, and drive cycles. Section III describes the paper’s simulation approach, and Section IV presents the main results and discusses the impact of battery size and control strategy on expected trip cost, expected efficiency, and state-of-charge range. The paper’s conclusions are provided in Section V.

Manuscript received August 1, 2008. This work was supported in part by the University of Michigan Rackham Merit Fellowship and National Science Foundation Graduate Research Fellowship.

S. J. Moura, H. K. Fathy, and J. L. Stein are with the Department of Mechanical Engineering, University of Michigan, Ann Arbor, MI 48109-2133 USA (e-mail: [sjmoura@umich.edu](mailto:sjmoura@umich.edu); [hfathy@umich.edu](mailto:hfathy@umich.edu); [stein@umich.edu](mailto:stein@umich.edu)).

D. S. Callaway is with the Center for Sustainable Systems in the School of Natural Resources and Environment, University of Michigan, Ann Arbor, MI 48109-1041 USA (e-mail: [dcall@umich.edu](mailto:dcall@umich.edu)).

## II. PHEV MODEL AND POWER MANAGEMENT ALGORITHM

This paper analyzes a hybrid vehicle model based upon the single mode power-split (a.k.a. parallel/series or combined) hybrid architecture in Fig. 1. The key benefit of the power-split design is that it possesses energy flow characteristics of both parallel and series configurations. The parallel flow paths include engine-to-wheels and battery-to-wheels (blue arrows), while the series flow path is from the engine-to-battery-to-wheels (red arrows). The role of the planetary gear set is to manage energy flow between these paths by transferring mechanical power between the engine, two motor/generators (identified as M/G1 and M/G2), and the wheels. An interesting result of this arrangement is that, with the appropriate control strategy, power can be split amongst the three paths to optimize energy consumption.

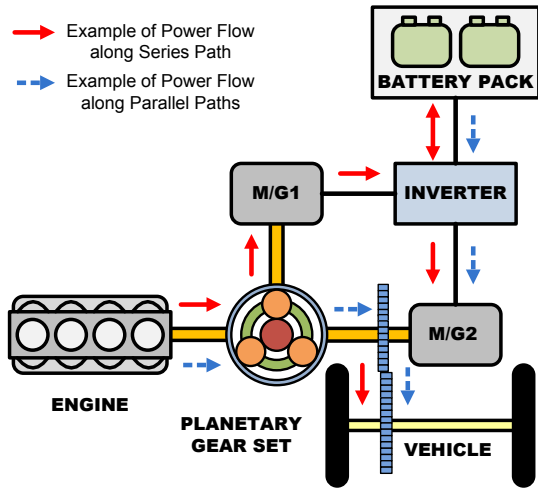


Fig. 1. The single mode power-split hybrid architecture uses a planetary gear set to split power amongst the engine, M/G1, and M/G2.

### A. PHEV Model

The vehicle model used in this paper was developed in previous work by the authors [7] and is largely based upon existing research on conventional hybrid electric vehicles (HEVs). The planetary gear set model utilizes Euler's Law to describe the inertial dynamics of the engine and motor/generators [8]. The engine and motor/generator models are steady-state maps, which relate speed and torque to fuel consumption and power efficiency [9].

Each nickel-metal hydride (NiMH) cell within the battery pack is modeled by an equivalent circuit comprising an ideal voltage source  $V_{oc,cell}$  in series with an Ohmic resistor  $R_{cell}$  [8], [10], where each cell has a charge capacity of  $Q_{cell}$ . Both the open circuit voltage and internal resistance are functions of battery state of charge (SOC). These equivalent circuits are assembled in a series-parallel combination to model the entire battery pack, where  $n_s$  denotes the number of cells in series per parallel string,  $n_p$  denotes the number of parallel strings, and the total number of cells in the pack is  $n_s n_p$ . The open circuit voltage  $V_{oc}$ , internal resistance  $R$ , and charge capacity  $Q$  for the entire battery pack are given by:

TABLE I  
PARAMETERS FOR PHEV MODEL

Parameter	Specifications
Vehicle Class	Midsized sedan
Vehicle Configuration	Single mode power-split
IC Engine Type	1.5L I4, Gasoline
Maximum Engine Power	43 kW
Maximum Engine Torque	102 N-m
M/G Type	Permanent Magnet AC
M/G1 Maximum Power	15 kW
M/G2 Maximum Power	35 kW
Battery Pack Chemistry	NiMH
Nominal Voltage	1.2 V per cell
Nominal Capacity	6.0 A-h per cell

$$V_{oc} = n_s V_{oc,cell} \quad R = \frac{n_s}{n_p} R_{cell} \quad Q = n_p Q_{cell} \quad (1)$$

The battery pack dynamics are associated with SOC, which intuitively describes a battery "fuel gauge". Here, we define SOC as the ratio of charge to maximum charge. As a result, the derivative of SOC is the ratio of current through the circuit  $I$  to an estimated maximum charge capacity  $Q$ .

$$\dot{SOC} = -I/Q \quad (2)$$

Through applying power conservation on the equivalent circuit, we obtain an expression for battery power at the terminals in (3). This expression may be written in terms of SOC and solved using the quadratic formula to obtain the equation for SOC in (4).

$$P_{batt} = V_{oc} I - R I^2 \quad (3)$$

$$\dot{SOC} = -\frac{V_{oc} - \sqrt{V_{oc}^2 - 4P_{batt}R}}{2QR} \quad (4)$$

Note that the battery model is scalable with respect to the number of NiMH cells. Although this formulation explicitly accounts for series-parallel cell architectures, it can be mathematically shown that, holding  $n_s n_p$  constant, the SOC dynamics are invariant to  $n_s$  and  $n_p$  individually. We will use this fact to avoid the need to specify the cell architecture. In practice, of course, pack voltage, inverter efficiency, heat generation, charge equalization, and state of health must all be considered in the battery design process [11], [12].

Although lithium-ion batteries are quite promising for PHEV applications, this paper's focus on NiMH batteries is still relevant, since many researchers currently build PHEVs by upgrading HEVs that utilize NiMH batteries. We will address the performance implications of Li-ion batteries in

future work.

The states for the assembled PHEV plant model include engine crankshaft speed  $\omega_e$ , longitudinal vehicle velocity  $v$ , battery state of charge  $SOC$ , and driver power demand  $P_{dem}$ . The controlled inputs to the plant include engine torque  $T_e$ , M/G1 torque  $T_{M/G1}$ , and M/G2 torque  $T_{M/G2}$ . Figure 2 shows that the state and control signals form a state feedback control loop around the PHEV model components.

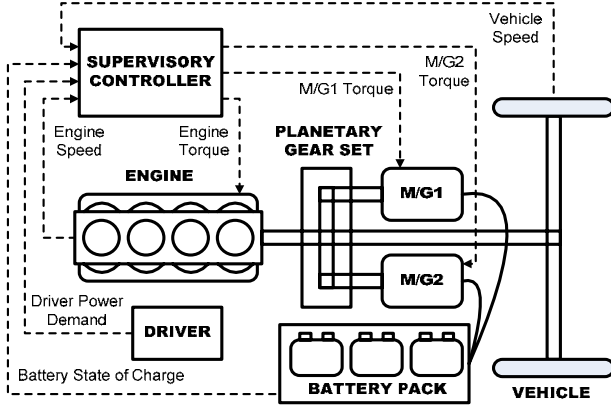


Fig. 2. PHEV model components and signal flow. Note that the signal flow forms a state feedback control architecture.

### B. Power Management Algorithm

In previous work, we developed optimal power management algorithms that minimize the combined consumption costs of fuel and electricity and can be implemented without prior knowledge of the trip characteristics, other than a stochastic power demand model [7]. Mathematically, the optimal control problem is summarized in the following infinite horizon formulation:

$$\text{Minimize: } J = \lim_{N \rightarrow \infty} \mathbb{E}_{P_{dem}} \left[ \sum_{k=0}^{N-1} \gamma^k g(x(k), u(k)) \right] \quad (5)$$

$$\text{Subject to: } x(k+1) = f(x(k), u(k)) \quad (6)$$

$$P_{i,j,m} = \Pr(P_{dem}(k+1) = i | P_{dem}(k) = j, v(k) = m) \quad (7)$$

$$P_{dem} = P_e + P_{M/G1} + P_{M/G2} \quad (8)$$

$$x \in X = \left\{ x : \begin{array}{l} \omega_{e,\min} \leq \omega_e \leq \omega_{e,\max} \\ \omega_{M/G1,\min} \leq \omega_{M/G1} \leq \omega_{M/G1,\max} \\ \omega_{M/G2,\min} \leq \omega_{M/G2} \leq \omega_{M/G2,\max} \\ SOC_{\min} \leq SOC \leq SOC_{\max} \end{array} \right\} \quad (9)$$

$$u \in U(x) = \left\{ u : \begin{array}{l} T_{e,\min} \leq T_e \leq T_{e,\max}(\omega_e) \\ T_{M/G1,\min} \leq T_{M/G1} \leq T_{M/G1,\max}(\omega_{M/G1}) \\ T_{M/G2,\min} \leq T_{M/G2} \leq T_{M/G2,\max}(\omega_{M/G2}) \\ P_{chg,\lim}(SOC) \leq P_{batt} \leq P_{dis,\lim}(SOC) \end{array} \right\} \quad (10)$$

where  $g(x(k), u(k))$  is the energy consumption cost per time step  $k$  and  $\gamma$  is the discount factor. The optimization is subject to both deterministic (6) and stochastic (7) model dynamics. The stochastic dynamics (7) take the form of a first order Markov chain in which  $P_{dem}$  is the Markov state variable. The constraint (8) ensures power demand is always met by the power sources. In (9) and (10),  $X$  is the set of admissible state values  $x$ , and  $U$  is the set of admissible control values  $u$ . The time step is one second. We use this framework to develop two separate control strategies, “blended” and “charge-depletion, charge sustenance” (CDCS):

1) *Blended*: The blended approach minimizes a weighted sum of fuel consumption and electric energy consumption

$$g(x, u) = \beta \alpha_{fuel} W_{fuel} + \alpha_{elec} \frac{1}{\eta_{grid}} P_{batt} \quad (11)$$

The parameter  $\beta$ , which we refer to as the “energy price ratio,” represents the price of gasoline per megajoule (MJ) relative to the price of electricity per MJ. The conversion factors  $\alpha_{fuel}$  and  $\alpha_{elec}$  are selected to convert energy consumption from each source to common units of MJ per time step.  $W_{fuel}$  is the fuel consumption rate in terms of grams per time step, and  $P_{batt}$  is power flow through the battery, which can be calculated from the battery pack open-circuit voltage, charge capacity and  $SOC$ .

$$P_{batt} = -V_{oc} Q \dot{SOC} \quad (12)$$

Note that  $P_{batt}$  is positive for discharge events and negative for regeneration events. We estimate the electric energy consumed from the grid during the recharge process by dividing  $P_{batt}$  by a constant charging efficiency  $\eta_{grid} = 0.98$ . For the main result in this paper we assume a fuel price ratio of  $\beta = 0.8$ , which is consistent with the average energy prices in the year 2006: \$2.64 USD per gallon of gasoline and \$0.089 USD per kWh of electricity [13]. However, we will also briefly report on results for other price ratios, and leave a more detailed analysis for a future publication.

2) *CDCS*: A common current practice for power management in PHEVs is to define two distinct modes, which this paper identifies as charge depletion and charge sustenance (CDCS) [5], [14], [15]. This method operates under the assumption that, in all power demand scenarios, fuel consumption operating costs dominate electricity consumption operating costs. Hence, CDCS depletes battery charge as fast as possible (engine power may be required to meet drivability requirements), and then uses the engine to regulate battery charge after reaching the minimum battery SOC. Here, we implement CDCS in the SDP framework, as suggested by [8], [16]-[19] by setting  $\alpha_{elec}$  in (10) equal to zero.

### C. Trip Duration Model

We model trip duration as a random variable  $T$ , whose distribution gives the total travel time for a vehicle during a single day, which we treat as the travel time between PHEV charging events. This model is based on data from the 2001 National Household Travel Survey (NHTS) conducted by the Department of Transportation (DOT) Federal Highway Administration (FHWA) [20]. Figure 3 shows the distribution of surveyed daily vehicle travel times, which has a mean of approximately 35 minutes and 75 percent of daily travel occurs in 32 minutes or less. The likely cause of the data's multi-modality is a tendency among survey participants to report trip duration in 5 minute increments. Since our intent is to randomly generate trip durations by inverting the trip duration cumulative distribution function (CDF), we compute the CDF and attenuate the modes with a five minute, uniformly weighted moving average in Fig. 4.

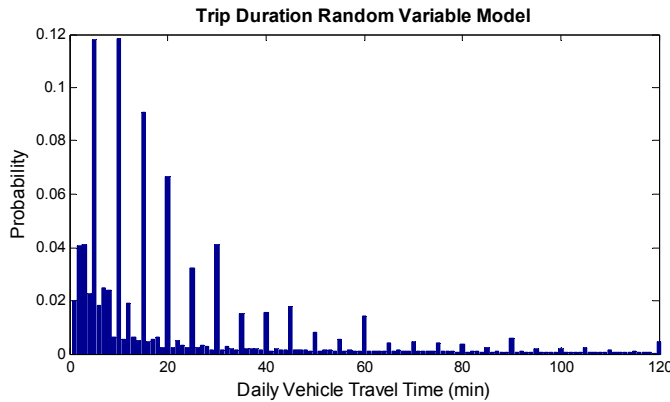


Fig. 3. Distribution of daily vehicle travel times from 2001 NHTS.

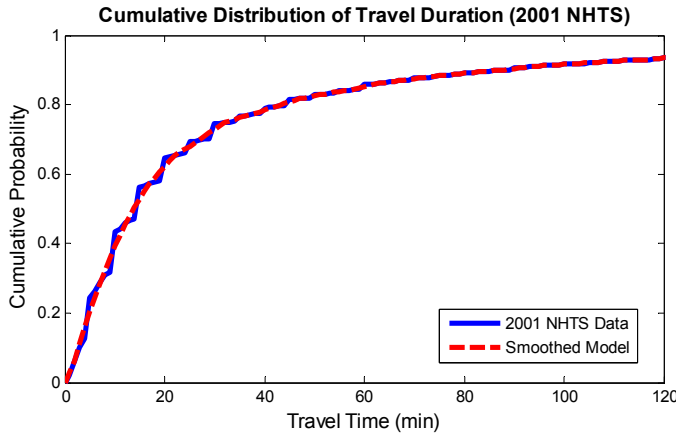


Fig. 4. Cumulative distribution of daily vehicle travel times.

### D. Drive Cycle Model

Drive cycle trajectories are modeled via a first order Markov chain, where power demand  $P_{dem}$  is the Markov state variable. This approach to modeling drive cycle trajectories is used widely in the hybrid vehicle power management literature [7], [8], [16], [17]. The transition probabilities for the Markov chain given by (7) are determined using a maximum-likelihood estimator [21] from observation data collected from federal drive cycles (FTP-

No. of Modules <sup>a</sup>	Battery Pack Energy Capacity	No. of Modules <sup>a</sup>	Battery Pack Energy Capacity
40	1.9 kWh	200	9.4 kWh
80	3.7 kWh	240	11.2 kWh
120	5.6 kWh	280	13.1 kWh
160	7.5 kWh	320	15.0 kWh

<sup>a</sup>Each module contains six (6) NiMH cells.

72, HWFET, US06) and real-world micro-trips (WVUCITY, WVUSUB, WVUINTER) in the ADVISOR database [9]. A sample randomly generated drive cycle is shown in Fig. 5. The Markov model assumes that the current state is conditioned only on the state immediately preceding it. We validated this assumption by computing the model residuals and confirming that their autocorrelation exceeds the 95 percent confidence interval for no more than 5 percent of all possible lag values – as is the case for a white noise process [22].

In the simulation method described below, we will assume that trip duration and the Markov model are independent. Although this is clearly an important assumption, there is limited data to test its validity, and we will leave it to future work to address the sensitivity of our results to the presence of drive cycle / trip duration dependence (e.g. longer trips tend to take place on the highway).

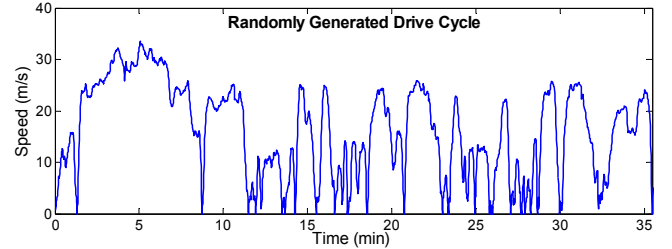


Fig. 5. A randomly generated drive cycle from the Markov chain model.

## III. SIMULATION METHOD

Distributions for the PHEV performance characteristics are calculated by simulating each control strategy (Blended and CDCS) and battery size (Table II) configuration over the entire distributions of trip duration and drive cycles. For each battery size option, we identify both a blended and CDCS control law (as explained in Section II-B and [7]). We then evaluate the performance of the control law / battery size combination by the following approach:

- 1) Sample a trip duration from the CDF in Figure 4.
- 2) Generate a power demand time series from the Markov chain model (7) with duration found in step 1.
- 3) Simulate the PHEV model on this randomly generated drive cycle and record the performance characteristics.
- 4) Check the stopping criterion (Appendix). If satisfied, stop simulations. If not satisfied, return to step 1.

## IV. RESULTS AND DISCUSSION

### A. Operating Costs & Energy Efficiency

Figures 6 and 7 show the distribution of operating costs (in USD per km) and energy efficiency (in MJ per km) for each battery size and control strategy configuration we examined. For batteries with fewer than 160 modules, the blended strategy is consistently superior to CDCS. In fact, we see that the distribution of operating costs and energy efficiency for the blended strategy is approximately the same as the distributions for CDCS, but with a larger battery size. For example, a blended strategy with a 120-module battery has roughly the same performance characteristics as a CDCS strategy with a 160-module battery. These results are in agreement with prior claims that a blended strategy should enable the use of smaller batteries [2], [4], [5].

It is important to note that the results shown here are for an energy price ratio of  $\beta = 0.8$ . As demonstrated in our previous work [7], the blended strategy converges to CDCS for very high price ratios. We re-ran the simulations shown in Fig. 6 and 7 for  $\beta = 2.0$  and found that the two strategies begin to converge, even for small battery sizes. Yet we observe no penalty for using the blended strategy, indicating that it remains appropriate for all  $\beta$ . However, its benefit cannot be fully quantified without knowledge of future  $\beta$  values.

The relative differences in median operating cost and energy efficiency between blending and CDCS become negligible as battery size increases. This relationship is related to the fact that neither control strategy enters charge sustenance mode for the vast majority of travel durations as battery size becomes sufficiently large. Instead, the power management algorithm remains in charge depletion mode, where blending and CDCS achieve nearly equal operating costs, as demonstrated in our previous research [7]. For extremely long travel durations, however, CDCS enters charge sustenance mode before the blending strategy and quickly accumulates elevated operating costs. This is the reason why the largest observations (upper whiskers in Fig. 6 & 7) for CDCS are consistently larger than the largest observations for blending.

As battery size increases, the operating costs and energy efficiency reach an asymptotic value. This result appears to imply that the daily payoff for purchasing PHEVs with very large batteries does not justify the higher acquisition cost at the time of purchase. Another way of interpreting this result is that for very large battery sizes (greater than 200 modules), it is very unlikely that the battery will fully deplete its charge because the bulk (75%) of daily trip durations are less than 35 minutes. However, batteries generally need to be oversized to minimize performance degradation over the lifetime of the vehicle. Although a smaller battery might reduce the purchase price of a PHEV, it may incur higher maintenance costs because it undergoes deeper discharge cycles that can accelerate power and

capacity fade [12].

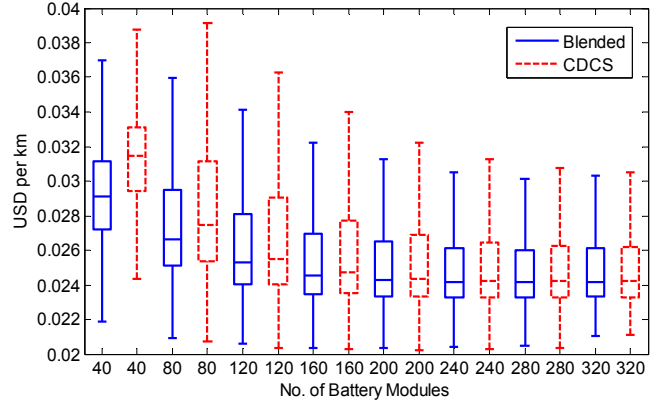


Fig. 6. Box and whisker plots of operating cost (USD per km) for each battery size and control strategy configuration. Whisker lengths are limited to 1.5 times the interquartile range.

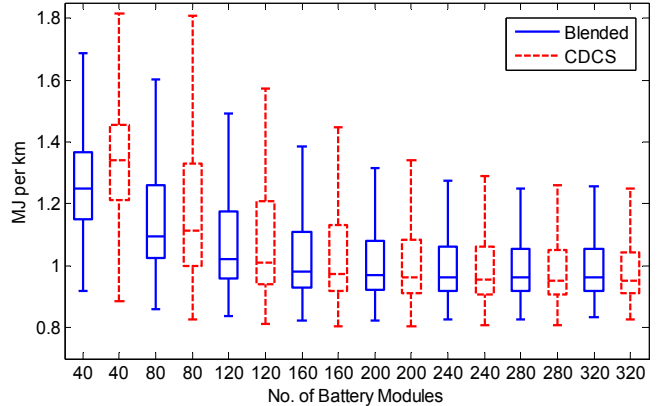


Fig. 7. Box and whisker plots of energy efficiency (MJ per km) for each battery size and control strategy configuration. Whisker lengths are limited to 1.5 times the interquartile range.

### B. SOC Range

To investigate the relationship between battery size and discharge depth, consider the distribution of SOC ranges shown in Fig. 8 for the two most extreme battery sizes. Here we define SOC range as the difference between the maximum and minimum SOC values achieved during the drive cycle. The asymptote at 0.65 occurs because the control strategy limits SOC between 0.25 and 0.9 using exterior point penalty functions (see [7]). The 40-module battery reaches full discharge depth in between 10 and 20 minutes, whereas the 320-module battery reaches full discharge depth in between 55 and 75 minutes. Within 10 to 20 minutes, only 35-60% of trips in one day have terminated. Therefore, in 40-65% of daily trips, a 40-module battery will reach full depletion. On the other hand, within 55 to 80 minutes, 84-90% of trips have terminated, meaning only 10-16% of PHEV daily trips will result in full depletion of a 320-module battery. Since this percentage is relatively small in comparison to the remainder of the population, the benefits of large battery sizes diminish as the number of modules increases.

Another way to interpret Fig. 8 is from a battery sizing

perspective. For example, suppose we wish to determine the battery size which achieves no more than a 0.5 SOC range during the first 75% of daily travel times. Reading off the cumulative probability curve, the first 75% of daily travel times corresponds to 32 minutes or less. Then we could populate Fig. 8 with the SOC range distribution for several battery sizes and determine which size achieves 0.5 SOC range or less for the first 32 minutes.

Eventually, it may make the most sense to treat PHEV battery size as an option on a vehicle, with smaller batteries standard (for those in the majority of the population with relatively low daily travel needs) and larger batteries available at a premium to those with greater travel requirements.

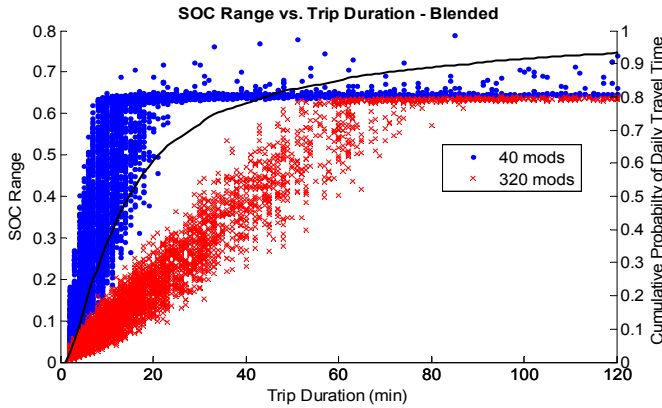


Fig. 8. Distribution of SOC range for 40 & 320 modules, blended strategy. The solid line is the cumulative distribution of daily travel time (Fig. 4). CDCS has a similar distribution and is therefore omitted for brevity.

## V. CONCLUSION

In this paper we have introduced a method for evaluating power management strategies and battery energy capacity in PHEVs. Through this framework, we have demonstrated that a blended control strategy facilitates the use of smaller batteries for a given operating cost or energy efficiency, with respect to a distribution of both daily travel time and drive cycles. We have also shown that expected operating cost and energy efficiency approach asymptotic values as battery size increases, since a very small population of drivers will fully deplete large batteries in one day. Because it is still not fully understood how the fundamental electrochemical properties of batteries affect PHEV performance and power management strategies, this paper has focused exclusively on optimizing energy cost. As scientific knowledge of PHEV battery performance and durability improve, it will be important to take these considerations into account.

## APPENDIX

The foundation for the stopping or convergence criterion is the central limit theorem (CLT) [23]. In this paper we seek convergence for the trip cost distribution. Suppose  $C_i$  is a random variable representing the trip cost

for the  $i^{\text{th}}$  simulation. Furthermore, suppose that the  $C_i$ 's are independently and identically distributed with mean  $E[C]$  and variance  $\sigma^2$  for the true population. The CLT allows us to approximate how many iterations  $n$  we must simulate the study in order that the sample mean is within a percentage  $a$  of the population mean with probability of at least  $b$ ,

$$\Pr\left(\left|\frac{1}{n}\sum_{i=1}^n C_i - E[C]\right|/E[C] \leq a\right) \geq b \quad (13)$$

Approximating the left-hand side of (2) using the CLT, one can show that this criterion is satisfied for

$$n \geq \left[\frac{\sigma_s}{m_s a} \Phi^{-1}\left(\frac{b+1}{2}\right)\right]^2 \quad (14)$$

where  $\Phi^{-1}$  is the inverse of the zero-mean, unit variance normal cumulative distribution function. The exact derivation of (14) requires knowledge of the population's mean  $m$  and standard deviation  $\sigma$ , however we approximate these values by the sample mean  $m_s$  and sample standard deviation  $\sigma_s$ . In practice, we run a minimum of 100 simulations before computing the stopping condition (14) in order to obtain a reasonably accurate estimate and avoid premature termination. The stopping criterion parameters used in this study are  $a = 0.05$  and  $b = 0.95$ .

## ACKNOWLEDGMENT

The authors thank Professor Huei Peng and Professor Zoran Filipi at the University of Michigan, Ann Arbor for their insightful comments and supportive guidance.

## REFERENCES

- [1] A. Simpson, "Cost-Benefit Analysis of Plug-in Hybrid Electric Vehicle Technology," presented at the *22nd International Battery, Hybrid and Fuel Cell Electric Vehicle Symposium and Exhibition EVS-22*, vol. NREL/CP-540-40485, 2006.
- [2] T. Markel and A. Simpson, "Energy storage systems considerations for grid-charged hybrid electric vehicles," *Proceedings of 2005 IEEE Vehicle Power and Propulsion Conference*, pp. 6 pp., 2005.
- [3] A. F. Burke, "Batteries and ultracapacitors for electric, hybrid, and fuel cell vehicles," *Proc. of the IEEE*, vol. 95, pp. 806-20, 04. 2007.
- [4] P. B. Sharer, A. Rousseau, S. Pagerit and P. Nelson. "Midsize and SUV vehicle simulation results for plug-in HEV component requirements." *SAE Papers 2007-01-0295*, 2007.
- [5] P. B. Sharer, A. Rousseau, D. Karbowski and S. Pagerit. "Plug-in hybrid electric vehicle control strategy: Comparison between EV and charge-depleting options," *SAE Papers 2008-01-0460*, 2008.
- [6] M. P. O'Keefe and T. Markel, "Dynamic programming applied to investigate energy management strategies for a plug-in HEV," *22nd International Battery, Hybrid and Fuel Cell Electric Vehicle Symposium, (EVS-22)*, 2006.
- [7] S. J. Moura, H. K. Fathy, D. S. Callaway, J. L. Stein, "A Stochastic Optimal Control Approach for Power Management in Plug-in Hybrid Electric Vehicles," to be published in *Proc. of 2008 Dynamic Systems and Controls Conference*, Ann Arbor, 2008.
- [8] J. Liu, H. Peng, "Modeling and Control of a Power-Split Hybrid Vehicle," *IEEE Transactions on Control Systems Technology*, to be published.

- [9] K. B. Wipke, M. R. Cuddy and S. D. Burch, "ADVISOR 2.1: A user-friendly advanced powertrain simulation using a combined backward/forward approach," *IEEE Transactions on Vehicular Technology*, vol. 48, pp. 1751-1761, 1999.
- [10] V. H. Johnson, "Battery performance models in ADVISOR," *Journal of Power Sources*, vol. 110, pp. 321-329, 2002.
- [11] M. Verbrugge and E. Tate, "Adaptive state of charge algorithm for nickel metal hydride batteries including hysteresis phenomena," *Journal of Power Sources*, vol. 126, pp. 236-249, 2004.
- [12] G. L. Plett, "Extended Kalman filtering for battery management systems of LiPB-based HEV battery packs. Part I. Background," *Journal of Power Sources*, vol. 134, pp. 252-61, 08/12. 2004.
- [13] Anonymous. (2007, Jun.). Annual Energy Review. U.S. Department of Energy. Tech. Rep. DOE/EIA-0384(2006). [Online]. Available: <http://www.eia.doe.gov/aer/>
- [14] A. Shabashevich, D. Saucedo, T. Williams, C. Reif, C. Lattoraca, B. Jungers, B. Wietzel, A. A. Frank. (2007, Apr.). "Consumer Ready Plug-in Hybrid Electric Vehicle," Team-Fate, University of California, Davis, CA. [Online]. Available: [http://www.team-fate.net/technical/UCDavis\\_Spring2007\\_TechReport.pdf](http://www.team-fate.net/technical/UCDavis_Spring2007_TechReport.pdf).
- [15] A. Rousseau, S. Pagerit, D. Gao, "Plug-in Hybrid Electric Vehicle Control Strategy Parameter Optimization", presented at *Electric Vehicle Symposium-23*, Anaheim, Calif., Dec. 2-5, 2007.
- [16] I. Kolmanovsky, I. Siverguina and B. Lygoe, "Optimization of powertrain operating policy for feasibility assessment and calibration: Stochastic dynamic programming approach," in *Proceedings of 2002 American Control Conference*, 2002, pp. 1425-30.
- [17] C.-C. Lin, "Modeling and control Strategy Development for Hybrid Vehicles," Ph.D. dissertation, Dept. of Mech. Eng., University of Michigan, Ann Arbor, MI, 2004.
- [18] E. D. Tate, "Techniques for Hybrid Electric Vehicle Controller Synthesis," Ph.D. dissertation, Dept. of Elec. Eng. an Comp. Sci., University of Michigan, Ann Arbor, MI, 2007.
- [19] L. Johannesson, M. Asbogard and B. Egardt, "Assessing the Potential of Predictive Control for Hybrid Vehicle Powertrains Using Stochastic Dynamic Programming," *IEEE Transactions on Intelligent Transportation Systems*, vol. 8, pp. 71-83, 2007.
- [20] Anonymous. (2001). National Household Travel Survey. [Online]. Available: <http://nhts.ornl.gov/index.shtml>
- [21] T. W. Anderson and L. A. Goodman, "Statistical inference about Markov chains," *Annals of Mathematical Statistics*, vol. 28, pp. 89-110, 1957.
- [22] P. J. Brockwell and R.A. Davis, *Time Series: Theory and Methods*, New York, NY: Springer, 1998.
- [23] J. A. Gubner, *Probability and Random Processes for Electrical and Computer Engineers*, New York, NY: Cambridge University Press, 2006, ch. 5.